

Post-print version of:

Publisher: **Taylor & Francis**

Journal paper: **Ships and Offshore Structures 2018, 14(3) 249-564**

Title: **Time Domain Simulator for Short-Term Ship Manoeuvring Prediction: Development and Applications**

Authors: **P. Neri**

Creative Commons Attribution Non-Commercial No Derivatives License



DOI Link: <https://doi.org/10.1080/17445302.2018.1496567>

RESEARCH PAPER

## Time Domain Simulator for Short-Term Ship Manoeuvring Prediction: Development and Applications

P. Neri<sup>a</sup>

<sup>a</sup>University of Pisa, Department of Civil and Industrial Engineering, Largo L. Lazzarino 1, Pisa, 56122 Italy

### ARTICLE HISTORY

Compiled June 29, 2018

### ABSTRACT

This paper presents a short-term time-domain algorithm for ship motion simulation. Plane motion is considered, thus a three degrees of freedom model can be used. The main inputs of the model are: propellers speed, rudder angles and initial conditions (in terms of initial position/orientation and linear/rotational velocity). The outputs are final ship position and orientation after a given simulation time. The huge amount of data available in the Voyage Data Recorder (VDR) and the results of sea trials performed before the ship delivery can be used to estimate the needed parameters, implementing a simple but reliable linear regression scheme. As a case study, the proposed model was applied to Costa Concordia manoeuvring simulation in order to assess its reliability in terms of trajectory prediction. Finally, as an example of application, the simulator was implemented in a real time manoeuvring predictor, which is capable of foreseeing the ship position up to 40 s ahead in time, supporting the Commander in emergency operations.

### KEYWORDS

Ship motion simulator; Plane motion model; Costa Concordia shipwreck; Manoeuvring predictor

## 1. Introduction

Simulating vessels' behaviour during navigation is a crucial issue for naval architects. Two different kinds of ship manoeuvring models are available in literature (23rd ITTC Manoeuvring Committee (2002)): models for prediction of ship manoeuvrability (a1) and models for use in simulators (a2). The a1 models are mainly aimed at estimating the vessel behaviour at design stage, in order to satisfy its compliance with technical specification and loyal requirements (International Maritime Organization, IMO). On the other hand, the a2 models are mainly developed for real-time or faster simulators for training purposes or to foresee the behaviour of a given ship (both at design stage or after ship construction). Since a1 simulators are generally set-up before vessels construction, a lot of information about design parameters need to be implemented in really complex models. Simulators exploiting a2 models instead are often based on less parameters, measured during PMM tests (if the model is developed before ship construction) or during sea trials (if the model is developed after ship construction). It is then possible to follow a sort of "black-box" approach. This approach is widely documented in literature; a mathematical model is built, setting its free parameters and coefficients

by means of a fitting process, using experimental data measured on the real system. Different choices can be made for the interpolation functions, such as polynomial, exponential or Gaussian functions, Maffezzoni and Gubian (1995). Moreover, recent techniques like neural network approximation have demonstrated their effectiveness in modelling complex systems, Poggio and Girosi (1990). In the case of ship position prediction, a simplified model can be studied and its parameters can be extracted from recorded navigation data to reflect the actual ship behaviour. A more detailed overview of the existing modelling techniques applied to ship manoeuvring simulation can be found in Sandaruwan et al. (2010); Suleiman (2000). In the present application, a least square fit was implemented to calculate the parameters needed by the chosen mathematical model. Two sources of experimental data were available for parameter extraction: the results of sea trials performed before the ship delivery to the owner and the data stored in the Voyage Data Recorder (VDR) during navigation.

Several publications are available concerning a1 models, which are really important for naval architects and ship designers and give good results in terms of manoeuvring evaluation, Revestido et al. (2011); Sutulo and amd C. Guedes Soares (2002); Oltmann (1996); Ishiguro et al. (1996). On the other hand fewer papers are available concerning a2 models, Barauskis and Friis-Hansen (2007); Shyh-Kuang et al. (2008). An example is given in Mohd et al. (2012), but the proposed simulator is not validated by means of comparison between simulated and experimental data. In Sandaruwan et al. (2010) the authors use an approach really similar to the one proposed in the present paper, i.e. a ship motion model is implemented based on few model parameters which are evaluated using standard ship manoeuvring tests. Anyway, a six-degrees of freedom model was implemented and complex equations of motion were used, also considering (uncertain) environmental conditions. Moreover, the parameters calculation was not explained in detail in Sandaruwan et al. (2010), and the authors stated that some parameters were approximated exploiting literature data. In the present paper, all the needed parameters were calculated from navigation data. The oil tanker ESSO Osaka was considered for validation in Sandaruwan et al. (2010), but simulation errors were pretty high: for instance, the experimentally measured turning radius was about 375 m while the simulated one was about 550 m.

This is the reason why a new simulator model was studied and presented in this paper. The model was applied during the trial for Costa Concordia shipwreck, to deeply investigate and reconstruct the instants before the impact with Giglio island rocks, Neri et al. (2014). Anyway, its application can be extended to other ships provided that the results of sea trials are known or a suitable set of recorded data is available. In Section 2 the implemented mathematical model is described, along with the main hypothesis and the numerical strategies adopted. The algorithm is then validated by means of comparison between experimental data and simulation results. The case study of the Costa Concordia is presented in Section 3. In Section 4 another application of the simulator is presented: since the proposed algorithm showed good results in terms of short term manoeuvres simulation, the simulator was implemented in a real time fashion for ship trajectory prediction, as a tool for Commander during emergency operations, Neri and Neri (2015). Finally, in Section 5 some conclusions are given, along with possible future developments of the proposed algorithms, such as the implementation in a control loop for auto-pilot applications or autonomous vehicles manoeuvring. Indeed, a reliable model of vehicle dynamics is a crucial issue to achieve control robustness, Bums (1995); Das and Talole (2016); McMahan and Plaku (2016).

## 2. Available data

The proposed approach requires the estimation of some model parameters through recorded navigation data. In particular, two sources of data were taken into account in the present application: standard sea trials results and regular navigation data stored in the VDR. In fact, some mandatory sea trials must be performed before the ship is delivered to the owner. Several international organizations are entitled to grant the manoeuvrability certificate (Manoeuvring Booklet). In the case of Costa Concordia these trials were performed by Centro per gli Sudi di Tecnica Navale (CETENA). The main tests performed on the vessel during sea trials are: Turning circle (steady state turning evaluation), Free stop (stopping distance evaluation), Crash stop (stopping distance evaluation if propellers are powered backwards), Zig-zag (evaluation of responsiveness to rudder position), Williamson turn (man overboard manoeuvre evaluation). These tests are performed using a Differential GPS, so that the positioning error is reduced to 2 m, and by recording the data on the VDR for successive elaboration.

On the other hand, VDR is a mandatory system installed on modern vessels to provide information to investigators in case of accident, International Maritime Organization (1997). Various sensors and devices record navigation data on an industrial grade computer (Picinelli and Gubian (2013), Gubian et al. (2015)). Among the data collected by the VDR, the most relevant for the present application are position (GPS error about 10 m), velocity, heading, date and time, propellers speed and rudders angle. Two hours of operation of the VDR after the loss of main power are guaranteed. At least a copy of the last 12 hours of recording is saved in the Final Recording Medium, which is a capsule designed to survive an accident and to be recovered by the investigators. Furthermore, a larger recording time can be provided by other supplementary recording media.

## 3. Mathematical model

The aim of the present work is to simulate the short-term behaviour of a ship in terms of heading and position. This problem is really complex in general, since ship response depends on several different parameters such as inertia properties, hull shape, propeller(s) type and rudder(s) dimension. Some simplifying hypothesis have been considered, in order to reduce model complexity and calculation time. For dynamics purpose, the ship can be considered as a 6 Degrees Of Freedom (DOF) rigid body. Anyway,  $z$  position and rolling and pitch angles are only relevant for stability studies and under severe weather conditions, while they can be neglected in this study. A 3 DOF model was then considered, as shown in Fig. 1.

This simple model proved to be adequate for short term prediction of the trajectory of the ship Maimun et al. (2011); Milanov et al. (2011); Skjetne et al. (2004). Moreover, it allowed to reduce the number of variables and equations involved, reducing simulation time without losing relevant information. In fact, neglected DOFs generally do not have relevant variations for cruise ship during travels (which is the case study presented in this paper), thus enhancing passengers comfort. This assumption anyway does not reduce the application field of the method, as it can be applied anytime plane motion is dominant in ship behaviour, e.g. big cargo ships, river boats and small boats travelling in calm water conditions (i.e. null wave excitation).

Another simplifying assumption is that wind and current effects are negligible for the considered manoeuvres. This effects have been modelled in other papers Pérez and Blanke (2002); Varela and Soares (2015); Raman-Nair et al. (2014), but the error introduced by neglecting

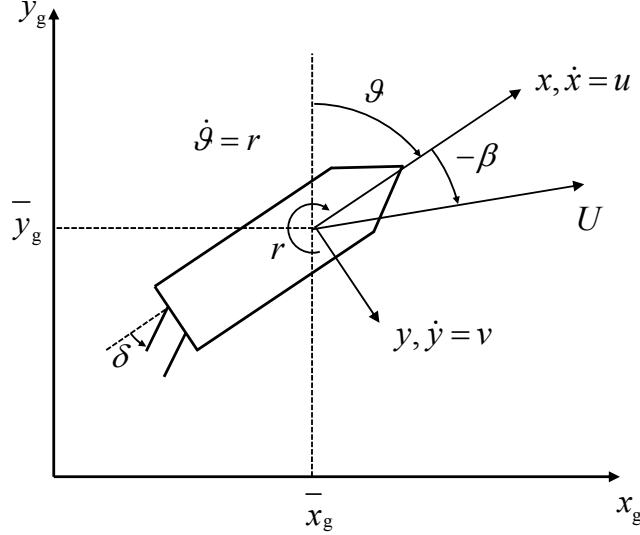


**Figure 1.** 3 DOF model and coordinate systems.

them is reduced if the simulated ship travels in calm water and low wind conditions, which is the case considered in the present paper.

The plane motion of the ship can then be studied considering Newton's equations among the three DOFs:

$$\begin{aligned}\ddot{\vartheta} &= \frac{M_z}{I_z} = \frac{1}{I_z}(M_\delta + M_r + M_p + M_e) \\ \ddot{x} &= \frac{F_x}{m} = \frac{1}{m}(F_u + F_p + F_{\delta,u} + F_{e,u} + F_{\vartheta,u}) \\ \ddot{y} &= \frac{F_y}{m} = \frac{1}{m}(F_v + F_{\delta,v} + F_{e,v} + F_{\vartheta,v})\end{aligned}\quad (1)$$

where  $M_\delta$ ,  $M_r$ ,  $M_p$  represent the yaw moment determined by the water interaction with the rudders, the hull and the propeller respectively, while  $M_e$  represents the effect of environmental conditions (i.e. wind and current).  $F_u$ ,  $F_p$ ,  $F_{\delta,u}$  are the hydrodynamic forces acting on the hull, on the propellers and on the rudders along the longitudinal direction.  $F_{e,u}$  represents the effect of environmental conditions along the longitudinal direction, while  $F_{\vartheta,u}$  represents the inertia force due to  $r = \dot{\vartheta}$ .  $F_v$  and  $F_{\delta,v}$  are the hydrodynamic forces acting on the hull and on the rudders along the transverse direction, while  $F_{e,v}$  represents the effect of the environmental conditions.  $F_{\vartheta,v}$  is the inertia force acting along the transverse direction. Finally,  $m$  represents the ship's mass and  $I_z$  represents its moment of inertia along the  $z$  axis. It is worth noting that, as stated, in this work environmental conditions such as wind and current were neglected, thus in the following  $M_e = 0$  and  $F_{e,u} = F_{e,v} = 0$ . Again, a complete representation of the loads acting on the ship would require a really deep knowledge of ship geometry and characteristics Maimun et al. (2013). Literature shows several papers which deal with this topic, providing high complexity solutions 21st ITTC Manoeuvring Committee (1996); 22nd ITTC Manoeuvring Committee (2002); 23rd ITTC Esso Osaka Specialist Committee (2002); Martelli et al. (2014). Those studies are surely useful during design stage, when ship's manoeuvrability must be evaluated before experimental data are available. The presented simulator is intended

to be applied to ships whose actual behaviour can be measured during navigation Sandaruwan et al. (2010). Those complicated relations can then be highly simplified, taking into account only the dependencies between the governing quantities. The simulator has been applied to Costa Concordia cruise ship, whose main characteristics are summarized in Tab.1.

**Table 1.** Main characteristics of Costa Concordia cruise ship

Quantity	Value	Unit
Length	289.6	m
Beam	35.5	m
Draft	8.4	m
Displacement	47000	t
Gross tonnage	114147	t

It has two independent engines connected to two independent propellers. A difference in the rotational velocity of the propellers can be set to facilitate turning manoeuvres. The ship also has two rudders with hydraulic actuators, which are always piloted to be parallel in the considered data. These considerations allowed to develop Eqs.1, which can be written as:

$$\begin{aligned}
 \ddot{\vartheta} &= N_1(\sin(\delta_1) + \sin(\delta_2))u|u| + N_2r|r| + N_3(p_1|p_1| - p_2|p_2|) \\
 \ddot{x} &= X_1(p_1|p_1| + p_2|p_2|) + X_2u|u| + X_3r^2 + X_4\ddot{\vartheta} \\
 \ddot{y} &= Y_1v|v| + Y_2\ddot{\vartheta} + Y_3r^2
 \end{aligned} \tag{2}$$

where  $X_i$ ,  $Y_i$ ,  $N_i$  represent constant coefficients, depending just on the considered vessel. The symbols  $p_1$  and  $p_2$  represent the propellers rotational velocity, and  $\delta_1$  and  $\delta_2$  represent the rudders angle (the subscript 1 refers to port side while the subscript 2 refers to starboard side). All the other symbols in Eqs.2 are referred in Fig.1. In the proposed model,  $\delta_1$  and  $\delta_2$  only appear in the first of Eqs. 2 through the constant parameter  $N_1$ . This implies that only the effect of the rudders on the rotational behaviour of the ship is considered at the present research stage (i.e.  $F_{\delta,u} = F_{\delta,v} = 0$ ). The action of the rudders mainly depends on the hydrodynamic force of the water, which can be considered proportional to the square of the velocity  $u$ . The hydrodynamic moment acting on the hull is represented by the term  $N_2r|r|$ . Finally, propellers influence on rotational behaviour is taken into account by the term  $N_3(p_1|p_1| - p_2|p_2|)$ :  $p_1$  and  $p_2$  appears with opposite signs because they produce opposite yaw moments on the hull. On the other hand, propeller speed appear as a sum (multiplied by  $X_1$ ) in the second of Eqs. 2, since both of them produce the same force sign in longitudinal direction. The hydrodynamic force acting on the hull is represented by the term  $X_2u|u|$ , and inertia terms are represented by  $X_3r^2$  (centrifugal component due to rotational velocity) and  $X_4\ddot{\vartheta}$  (tangential component due to rotational acceleration). Finally, only the hydrodynamic force acting on the hull and inertia effects are considered to be relevant in the third of Eqs. 2 and are represented with the terms  $Y_1v|v|$  and  $Y_2\ddot{\vartheta} + Y_3r^2$  (sum of centrifugal and tangential components) respectively.

These equations could not be used in ‘‘a priori’’ model because of the high simplification level and the difficulties to directly obtain the values of the needed constant parameters at design stage. This simplification anyway is compensated in the proposed simulator by the experimental constant parameters, which are extracted using recorded navigation data: the model is trained using known data to learn how the ship would behave under certain inputs. Nevertheless, a more refined mathematical model could take into account some other dependencies, improving the simulation reliability (also for longer time) and enhancing the application field

of the method. Some possible model development are proposed in the conclusions.

### 3.1. Parameters extraction

This section describes how the constant parameters needed to integrate the equations of motion (Eqs.2) can be calculated using manoeuvring data collected during sea trials. In this paper, Costa Concordia cruise ship was used as a case study. Two main data sources were available: manoeuvring booklet and VDR registrations.

The manoeuvring booklet is an official report which describes the results of standard manoeuvres of the studied ship in terms of rudder angles, propeller speed, east and north coordinates and heading. The tests are aimed at verifying if the ship response to the given command is compatible with the specifications. Anyway, these experimental data can be directly used only to analyse manoeuvring instructions (i.e. propellers speed and rudders angle) which are really close to the test ones. It is not possible to estimate the ship answer in different conditions directly from those results. On the other hand, it is possible to use recorded data to estimate the values of the constant parameters needed in Eqs.2. Those parameters can then be used to estimate the ship response under arbitrarily chosen inputs.

The parameters extraction algorithm can be exemplified considering the first of Eqs.2. All the time-varying quantities ( $\delta$ ,  $u$ ,  $r$ ,  $p_1$ ,  $p_2$ ) are known in the chosen recorded data (i.e. VDR or CETENA data), while the constant parameters are the unknowns ( $N_1$ ,  $N_2$ ,  $N_3$ ). The first of Eqs.2 can be rearranged in a matrix form as follows:

$$M_{\vartheta} = \begin{bmatrix} (\sin(\delta_1(t_1)) + \sin(\delta_2(t_1)))u(t_1)|u(t_1)| & r(t_1)|r(t_1)| & (p_1(t_1)|p_1(t_1)| - p_2(t_1)|p_2(t_1)|) \\ \dots & \dots & \dots \\ (\sin(\delta_1(t_i)) + \sin(\delta_2(t_i)))u(t_i)|u(t_i)| & r(t_i)|r(t_i)| & (p_1(t_i)|p_1(t_i)| - p_2(t_i)|p_2(t_i)|) \\ \dots & \dots & \dots \\ (\sin(\delta_1(t_n)) + \sin(\delta_2(t_n)))u(t_n)|u(t_n)| & r(t_n)|r(t_n)| & (p_1(t_n)|p_1(t_n)| - p_2(t_n)|p_2(t_n)|) \end{bmatrix}$$

$$\begin{bmatrix} \ddot{\vartheta}(t_1) \\ \dots \\ \ddot{\vartheta}(t_i) \\ \dots \\ \ddot{\vartheta}(t_n) \end{bmatrix} = M_{\vartheta} \begin{bmatrix} N_1 \\ N_2 \\ N_3 \end{bmatrix} \quad (3)$$

The considered system is overdetermined, since it has a number of equations equal to the number of recorded data, thus much higher than the number of parameters to be computed. The problem can then be solved by means of a least square interpolation. It can be proven that the least square solution of the problem can be found by computing the pseudoinverse matrix Lawson and Hanson (1995). If a matrix  $A$  is considered, having  $n$  rows and  $m$  columns ( $n \geq m$ ), its pseudoinverse  $A^+$  is defined as:

$$A^+ = (A^T A)^{-1} A^T \quad (4)$$

Eq.3 can then be solved to find the parameters  $N_i$  by computing  $M_{\vartheta}^+$ :

$$\begin{bmatrix} N_1 \\ N_2 \\ N_3 \end{bmatrix} = M_{\vartheta}^+ \begin{bmatrix} \ddot{\vartheta}(t_1) \\ \dots \\ \ddot{\vartheta}(t_i) \\ \dots \\ \ddot{\vartheta}(t_n) \end{bmatrix} \quad (5)$$

This procedure can be applied to all the equations of motion (Eqs.2), so that all the needed parameters  $N_i$ ,  $X_i$ ,  $Y_i$  can be computed (see Appendix A for the regression analysis results). Several different recorded manoeuvring data were considered in this work as a reference to calculate the constant parameters. The CETENA sea trials data were considered to be more reliable to extract the parameters, due to the higher accuracy of the differential GPS system adopted to record data. Thus, the Turning circle manoeuvre documented in the CETENA Manoeuvring Booklet was firstly adopted to compute parameter Set1. Anyway, to assess the effect of low-quality data on parameters extraction, also VDR data (measured with on board GPS system) recorded just before the impact with the Giglio island's rocks were considered to extract a parameter Set2. This allowed to confirm that the higher quality of the Manoeuvring booklet data was crucial to obtain a reliable parameter set (see below).

### 3.2. Initial conditions

After parameters estimation, Eqs.2 can be integrated. Anyway, the integration process needs as an input the initial conditions of the ship at the simulation starting time, i.e. initial coordinates and heading (which will be called “initial position” for brevity) and linear and rotational velocities (which will be called “initial velocity”).

Initial conditions estimation is not trivial: the VDR records information about ship's velocity (both linear and rotational), but these values are not highly reliable since sensors precision is low. Moreover, only the amplitude of the resultant vector is measured, giving no information about its two plane components ( $u$ ,  $v$ , Fig.1). Velocity information could then be obtained by deriving recorded coordinates and heading with respect to the time, but a numerical incremental ratio would give an unstable result, because of GPS and compass measurement noise. To overcome this issue, position and orientation information of the ship were interpolated with a polynomial function. A third order form was chosen, thus the acceleration is time dependent. The  $q$  generic DOF of the ship (i.e.  $x_g$ ,  $y_g$  or  $\vartheta$ ) could be written in the form:

$$q(t) = at^3 + bt^2 + ct + d \quad (6)$$

where  $a$ ,  $b$ ,  $c$  and  $d$  represent the polynomial coefficients. Being  $t_0$  the simulation starting time, a time window was cut around  $t_0$  from the imported data, having a length  $2t_w$  (e.g.  $t_w = 10$  s in the following). The data belonging to the range interval between  $t_0 - t_w$  and  $t_0 + t_w$  were considered to calculate the coefficients in Eq.6 using a least square fit. It was then possible to derive the polynomial form to obtain the velocity information (i.e.  $\dot{q}(t) = 3at^2 + 2bt + c$ ). This procedure was applied to the 3 DOF of the ship as defined in Fig.1. Fig.2 shows an example of the VDR recorded ship's  $x_g$  coordinate over time (black dots). The gray solid line represents the computed polynomial, while the dashed black line represents the tangent obtained using the described method.

It is worth noting that the described procedure returns the best initial velocity estimation at

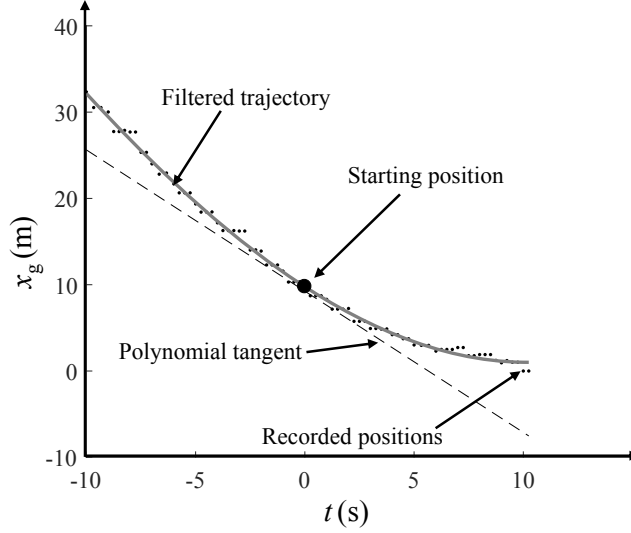


**Figure 2.** Initial conditions estimation through polynomial filtering.

the middle point of the studied interval and it is applicable only if a manoeuvre recorded in the VDR is to be simulated. On the other hand, if the simulator is implemented in a prediction algorithm for real time application (see below) no information are available after  $t_0$ . In this situation, the time window used for the interpolation is  $t_0 - 2t_w$ , and the best estimation of initial velocity is obtained at  $t_0 - t_w$ . The first  $t_w$  s of simulation are then used to compute velocity information at  $t_0$ , while the new foreseen data will start at  $t_0$ .

### 3.3. Differential equations integration

Differential equations integration is the last step to obtain the simulated ship trajectory and its final position and heading. Two different integration methods were considered for the application, Epperson (2013): forward Euler's method and Runge-Kutta method. While the first requires a simpler implementation and a shorter computational time, the latter is known to provide better performances by means of integration error over time. The two methods showed almost equal integration results: since mainly short time simulations are performed in the present work, the advantages of the more complex Runge-Kutta method were found to be negligible for this application. On the other hand, the forward Euler's method was found to be four times faster than the Runge-Kutta method. Thus, the simpler forward Euler's method was selected, using a time step  $d_t = 0.1$  s. In each time step, the first of Eqs.2 is independent from the others, so it could be integrated first (considering the accelerations expression of Eq.2):

$$\begin{aligned} \dot{v}_{i+1} &= \dot{v}_i + \ddot{v}_i d_t \\ v_{i+1} &= v_i + \dot{v}_i d_t + \frac{1}{2} \ddot{v}_i d_t^2 \end{aligned} \quad (7)$$

The  $x_g$  and  $y_g$  coordinates needed a more articulated procedure instead, since the reference frame chosen to write the equations of motion was not fixed (Fig.1). From the second and third of Eqs.2, accelerations along  $x$  and  $y$  local directions could be obtained, thus the module of

resultant acceleration vector was  $a = \sqrt{\ddot{x}^2 + \ddot{y}^2}$ . It was then possible to compute  $\ddot{x}_g = a \sin(\gamma)$  and  $\ddot{y}_g = a \cos(\gamma)$ , being  $\gamma = \arctan(\ddot{y}/\ddot{x}) + \vartheta$  the angle between the acceleration vector and the  $y_g$  direction. The forward Euler's method could be used to compute  $u, v$ :

$$\begin{aligned} u_{i+1} &= \dot{x}_{i+1} = \dot{x}_i + \ddot{x}_i d_t \\ v_{i+1} &= \dot{y}_{i+1} = \dot{y}_i + \ddot{y}_i d_t \end{aligned} \quad (8)$$

Then, considering that  $U = \sqrt{u^2 + v^2}$  and  $\beta = \arctan(-v/u)$ , it is possible to find  $\dot{x}_g, \dot{y}_g$ :

$$\begin{aligned} \dot{x}_{g,i} &= U_i \sin(\beta_i + \vartheta_i) \\ \dot{y}_{g,i} &= U_i \cos(\beta_i + \vartheta_i) \end{aligned} \quad (9)$$

Finally, the coordinates  $x_g, y_g$  of the ship can be determined as:

$$\begin{aligned} x_{g,i+1} &= x_{g,i} + \dot{x}_{g,i} d_t + \frac{1}{2} \ddot{x}_{g,i} d_t^2 \\ y_{g,i+1} &= y_{g,i} + \dot{y}_{g,i} d_t + \frac{1}{2} \ddot{y}_{g,i} d_t^2 \end{aligned} \quad (10)$$

At the end of each time-step, final  $x_g$  and  $y_g$  coordinates and heading  $\vartheta$  were obtained, along with additional information such as  $u, v$  and  $r$  velocities and  $\beta$  angle. It was then possible to simulate an arbitrarily long time period by repeating the described procedure iteratively.

### 3.4. Algorithm description

This paragraph summarizes how the proposed model was implemented in an algorithm to simulate the ship behaviour. Firstly, recorded navigation data sets are imported from VDR, manoeuvring booklet or other sources. Then, the constant parameters of Eqs.2 are estimated from the chosen set of known data. This operations can be performed just once, and then the obtained parameters can be used for all the desired simulations. Once simulator setup is completed, initial conditions are calculated with the polynomial interpolation described above. Rudders angle and propeller power are programmed for the whole simulation time. Differential equations are integrated for the chosen simulation time. The algorithm outputs are then available in terms of position, velocity and acceleration along the 3 DOFs over time, and can be plotted for post-processing purposes. Fig.3 shows the steps of the proposed algorithm.

### 3.5. Model validation

The described algorithm was validated by comparing simulation data with measured ones. Ship's initial conditions were extracted from recorded data, along with rudder angles and propellers speed, then simulations started. Finally, simulated results were compared with real measured ones.

To better validate the results, both considered sets of parameter values (i.e. Set1 and Set2) were firstly applied to simulate the same manoeuvre they were extracted from. Then, both

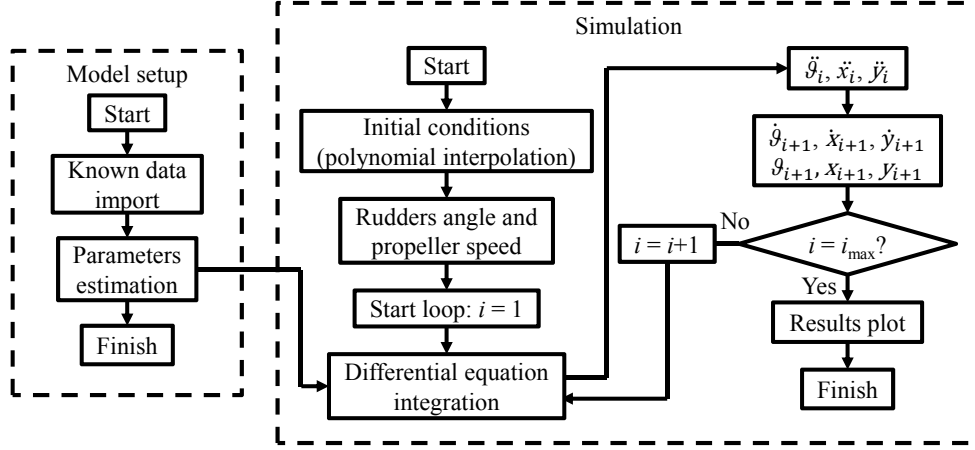


Figure 3. Algorithm flow chart: parameters extraction and simulation procedure.

Set1 and Set2 were used to simulate some manoeuvres which were totally independent from the ones used to extract the parameter sets. The same independent manoeuvres were used to validate Set1 and Set2, in order to compare simulator performances obtained by using different parameter sets, computed exploiting data sources with different accuracy levels.

This procedure was firstly applied to Manoeuvring Booklet data. Three main manoeuvres were considered: Turning circle ( $35^\circ$ , manoeuvre C1), Zig-Zag ( $\pm 10^\circ$ , manoeuvre C2) and Williamson turn (manoeuvre C3). Set1 was finally extracted using the full manoeuvre C1 with the proposed least square fit: the details of the regression analysis for  $\dot{\vartheta}, \dot{x}, \dot{y}$  are reported in Appendix A. Set1 was then applied to the simulation of C1, C2 and C3. The results of these three simulations (300 s of simulation time) are reported in Fig.4. The grey line in Fig.4 represents the full manoeuvre as recorded in the VDR, while the black dashed line represents the portion of the recorded manoeuvre which was simulated for validation. The black solid line represents the simulated trajectory, which as to be compared with the black dashed line. More precisely, Fig.4(b) shows that the model is able to properly reproduce a Zig-Zag manoeuvre even if its parameters are extracted from a constant turning manoeuvre. Furthermore, Fig.5 shows the simulated time series obtained by using parameter Set1 to simulate the Turning Circle manoeuvre (i.e. C1, Fig.4(a)), proving a good correspondence for the whole simulation time. Results can be considered surprisingly good, considering the simplicity of the model used and the few information required to build it (i.e. no design parameters are needed, but just data recorded during the sea trials). It is worth noting that the parameter Set1, extracted from the steady manoeuvre C1, was also successfully adopted to simulate the unsteady manoeuvres C2 and C3, as shown in Fig.4(b) and Fig.4(c).

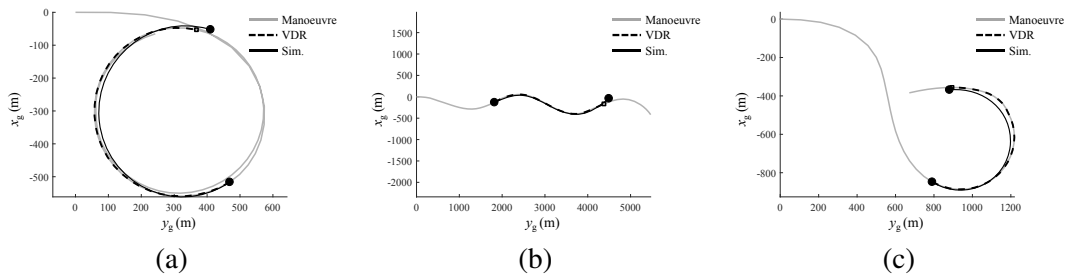
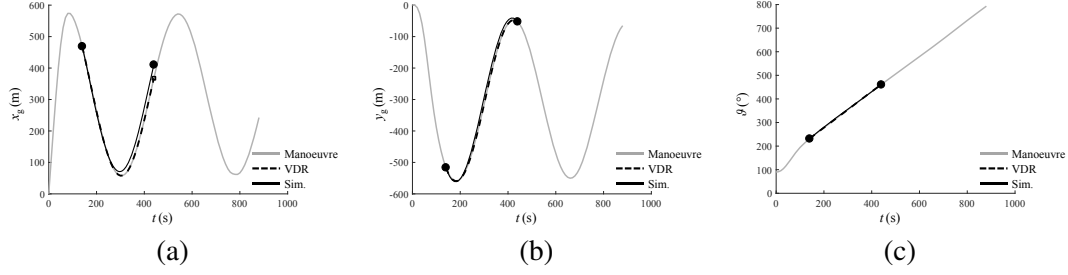


Figure 4. Simulation results obtained by using parameter Set1 (300 s): (a) Turning circle (C1) (b) Zig-zag (C2) and (c) Williamson turn (C3).



**Figure 5.** Turning circle simulated time series (Set1, 300 s): (a)  $x_g$  coordinate (b)  $y_g$  coordinate and (c)  $\vartheta$  heading.

Set2 parameters were extracted using VDR navigation data recorded just before the Costa Concordia impact with the rocks (manoeuvre V1). This choice was made because the proposed model neglects weather conditions and uses simplified relations to estimate the forces acting on the ship. Moreover, sea trials used to extract the parameters of Set1 were performed with no load on the ship (passengers, materials etc.) and by using regular trajectories (like turning circles), whereas before the impact the ship was loaded by more than 4000 passengers and the trajectory was quite irregular due to the continuous position changes of the rudders ordered by the Commander. Therefore, it was decided to extract the parameters also from a manoeuvre (V1) which was as close as possible to the simulation conditions (it is worth noting that the initial aim of the simulator was for use during trial at the court of Grosseto in order to evaluate the effects of the manoeuvres performed just before the shipwreck). Nevertheless, it is worth noting that VDR navigation data were recorded with really lower accuracy with respect to manoeuvring booklet data, thus they were considered less reliable in parameter estimation. Indeed, parameter Set2 was considered for comparison purposes only, to confirm that the data accuracy is crucial in determining realistic parameters.

Both the parameter sets were then also tested on some manoeuvres recorded in Costa Concordia VDR during the week ending with the shipwreck. Three particular events of the navigation were selected for validation: Giglio Impact (which corresponds to manoeuvre V1, few seconds before the impact), Palamos Turn (V2) and Palma Zig-Zag (V3); the name were assigned because of the site in which they occurred and the manoeuvre typology. Different simulation time intervals were chosen for manoeuvres V2 and V3, in order to understand how simulator's reliability evolves with respect to simulation time. In the case of V1 only a simulation time of 20 s was considered, thus the effect of a helmsman's error which occurred about 20 s before the impact could be evaluated. Tables 2, 3 report a comparison between the simulations performed for manoeuvres V1, V2, V3 using parameter Set1 and Set2 for increasing simulation time (the symbols are referred in Fig.1). These results show that the simulator is very reliable for a simulation time of about 40 s, when parameter Set1 is used: positioning errors are lower than 6 m and heading errors are about  $1^\circ$ . Tables 2, 3 also show percentage errors for  $x$  and  $y$  coordinates, which represent the relative error along those two directions with respect to the total distance traveled by the ship during the simulation time. As can be noted, this error is lower than 3 % for all the performed simulations (up to 80 s of simulation). On the other hand, parameter Set2 gives worst results, showing an heading error close to  $4^\circ$  for 40 s simulations, and even higher for longer simulations. Also, a relevant error along the  $x$  direction can be noted, e.g. in V2 and V3 manoeuvre. This confirmend that the higher quality of the data used to extract parameter Set1 was crucial in determining reliable parameters. Concerning manoeuvre V1, error evaluation could only be performed for a simulation time of 20 s, since the impact with the rocks occurred after that simulation time. The absolute errors considerably increase if simulation time exceeds 1 minute. This was considered acceptable for the purposes of the present work, since only short-term simulations were considered. As simulation time increases, environmental conditions (which are neglected in the model) play a

relevant role in ship's behaviour. Moreover, the forward Euler's integration method causes an error which increases over time, so that long-term simulations are not reliable. It is also worth noting that parameter Set1 returns better results in terms of simulation error, as expected. This is probably due to the fact that Set1 is computed using sea trials data, measured using a differential GPS system. Parameter Set2 is computed using VDR data instead, measured using the ship's on board GPS system. The error of the differential GPS is really lower than the error of the ship's GPS system, so that the positioning data are more precise and more suitable to compute the parameter set. This confirmed that the higher quality of the manoeuvring booklet data is crucial to achieve reliable simulation parameters. Also, the data used to compute Set1 and Set2 were acquired under different loading conditions. Anyway, the presence of the passengers represents a second order effect since the total load determined by 4000 passengers could be estimated around 400 t, which is less than 1% of the total ship displacement of 47000 t, as reported in Tab.1. Finally, results obtained using Set1 to simulate the manoeuvre V1 are also reported in Fig.6, to graphically show the quality of the simulated results with respect to the actual recorded data. Moreover, the graphical comparison between measured and simulated data obtained using Set1 to simulate manoeuvre V2 and V3 are reported in Appendix B.

**Table 2.** Simulation errors for increasing simulation time (parameter Set1).

<b>Giglio Impact (V1)</b>					
<b>Sim. time (s)</b>	<b><math>x_g</math> (m)</b>	<b><math>x</math> %</b>	<b><math>y_g</math> (m)</b>	<b><math>y</math> %</b>	<b><math>\vartheta</math> (°)</b>
20	-0.2	-0.13	5.4	3.71	0.11
<b>Palamos Turn (V2)</b>					
<b>Sim. time (s)</b>	<b><math>x_g</math> (m)</b>	<b><math>x</math> %</b>	<b><math>y_g</math> (m)</b>	<b><math>y</math> %</b>	<b><math>\vartheta</math> (°)</b>
20	-0.7	-0.41	-2.2	-1.23	-0.32
40	3.2	0.88	1.4	0.39	-1.10
80	2.6	0.37	-21.2	-2.96	-5.14
<b>Palma Zig-Zag (V3)</b>					
<b>Sim. time (s)</b>	<b><math>x_g</math> (m)</b>	<b><math>x</math> %</b>	<b><math>y_g</math> (m)</b>	<b><math>y</math> %</b>	<b><math>\vartheta</math> (°)</b>
20	0.0	0.00	-1.1	-1.14	-0.04
40	-0.9	-0.50	-3.0	-1.55	0.09
80	-4.6	-1.20	-11.2	-2.93	0.13

**Table 3.** Simulation errors for increasing simulation time (parameter Set2).

<b>Giglio Impact (V1)</b>					
<b>Sim. time (s)</b>	<b><math>x_g</math> (m)</b>	<b><math>x</math> %</b>	<b><math>y_g</math> (m)</b>	<b><math>y</math> %</b>	<b><math>\vartheta</math> (°)</b>
20	-3.9	-2.74	4.8	3.32	-3.50
<b>Palamos Turn (V2)</b>					
<b>Sim. time (s)</b>	<b><math>x_g</math> (m)</b>	<b><math>x</math> %</b>	<b><math>y_g</math> (m)</b>	<b><math>y</math> %</b>	<b><math>\vartheta</math> (°)</b>
20	-0.1	-0.08	-1.5	-0.86	-0.72
40	6.5	1.80	2.5	0.70	-2.52
80	23.8	3.32	-23.9	-3.33	-10.61
<b>Palma Zig-Zag (V3)</b>					
<b>Sim. time (s)</b>	<b><math>x_g</math> (m)</b>	<b><math>x</math> %</b>	<b><math>y_g</math> (m)</b>	<b><math>y</math> %</b>	<b><math>\vartheta</math> (°)</b>
20	0.7	0.69	-0.8	-0.85	-0.38
40	2.1	1.07	-1.8	-0.95	-1.36
80	11.0	2.88	-8.2	-2.13	-4.7

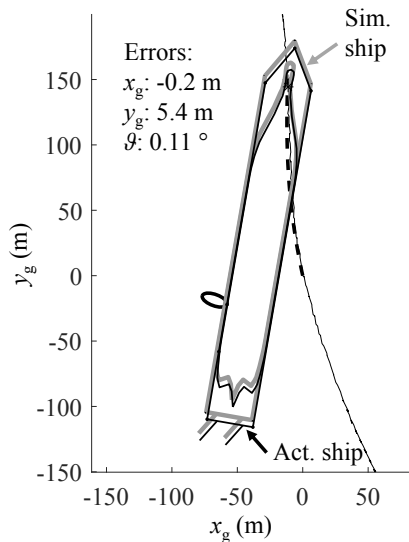


**Figure 6.** Results for Giglio impact simulation (Set1, V1, 20 s).

#### 4. Costa Concordia shipwreck simulation

The previous paragraph showed the performances of the proposed simulator in terms of ship trajectory prediction. The simulator was then applied to the Giglio island accident occurred to Costa Concordia cruise ship on January 13th 2012. During the trial it has been proved that Commander Schettino ordered a “hard to port” manoeuvre about 20 seconds before the impact, which was misunderstood by the helmsman who put the helm “hard to starboard” instead. The simulator was then used to evaluate the effect of this error on the ship trajectory close to the rocks. To do so, both Set1 and Set2 were firstly used to simulate the actual manoeuvre, which includes the helmsman’s error. The previous paragraph reports the obtained results (Tab.3 and Fig.6), which show a small error lower than 6 m for position and about  $0.1^\circ$  for heading using Set1 (and about  $3.5^\circ$  for heading using Set2). Subsequently, the audio file recorded in the VDR was used to reconstruct the exact command sequence ordered by the Commander, and simulations were repeated both for Set1 and Set2 removing the helmsman’s error. Fig.7 shows the results obtained using Set1.

The result is that at 21:45:11, which is the reconstructed impact time as recorded in the VDR, no impact occurs neither for the simulation (removing the helmsmen’s error) obtained using Set1 or Set2. According to Set2 results, the impact is fully avoided, as the ship passes about 16 m far from the rocks. Anyway, results obtained with Set2 are generally less reliable than the ones obtained using Set1, which provides the most conservative predictions, representing the worst case instead. Using Set1, the impact is delayed in time, so that the rocks impact the hull 18.5 m behind the actual impact location. This means that at least one machine room (more likely both of them) could be left undamaged by the impact, so the ship could still stay afloat, supplied by energy and responsive to the subsequent commands. Furthermore, it is possible to consider the rotational velocity of the ship at the impact instant. In the simulation with the helmsman’s error, the final rotational velocity of the ship at impact time is about  $0.56^\circ/s$ . In the simulation with no helmsman’s error, the final rotational velocity is about  $0.27^\circ/s$ , i.e. halved with respect to the simulation which considers the helmsman’s error. This means that, in the described worst case scenario, if the helmsman did not misunderstand the Commander’s order, the rotational energy could be reduced to the 25 % of the actual one (rotational energy is proportional to the square of the rotational velocity), probably

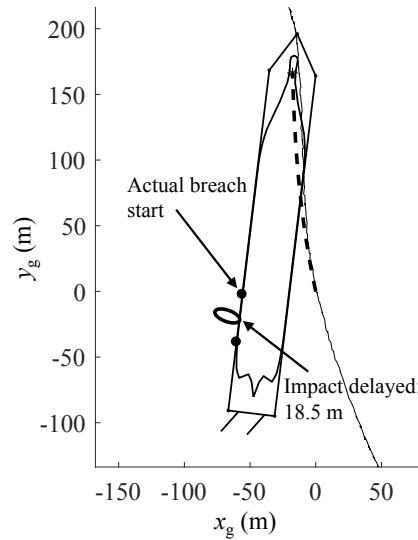


**Figure 7.** Simulation results for Giglio manoeuvre without the helmsman's error (Set1).

strongly reducing the impact catastrophic effects. Anyway, in order to assess the actual effects of the helmsman's error, these results should be verified through offshore experimental analysis performed on a similar ship (e.g. the twin ship Costa Serena), by comparing the ship trajectories with and without the helmsman's error.

It is worth noting that these results also show that, even though the ship motion is highly influenced by inertia forces, the time sequence of the commands imparted to propellers and rudders has a strong effect in ship behavior even for short simulation times. In fact, the ship behavior with the modified control sequence (i.e. without the helmsman's error) is highly different from the behavior corresponding to the recorded data, especially regarding the heading  $\vartheta$ .

## 5. Simulator implementation in a manoeuvres prediction algorithm

Since the simulator showed to have good performances in terms of ship's trajectory estimation, it was implemented in a real time fashion as a manoeuvre predictor. More precisely, parameter Set1 was used, because of its better performances in terms of simulation errors. The values of the parameters are reported in Tab.4: the numerical values and their units are valid if in Eqs.2 linear velocities and accelerations are expressed in m/s and  $m/s^2$  respectively, angular velocity and acceleration are expressed in rad/s and  $rad/s^2$  respectively and propellers speed is expressed in rpm.

The proposed algorithm is capable to foresee the ship trajectory up to 40 s ahead in time, displaying a real time estimation of the effect of the ordered manoeuvres on electronic charts on the bridge. The algorithm can run with the chosen frequency (in the following, 1 Hz frequency is used), using the Personal Computer available in the on board Integrated Navigation System.

### 5.1. Algorithm description

As already mentioned, the algorithm runs in real time. At the beginning of each cycle ( $t = t_0$ ) it firstly computes initial conditions, using the procedure explained above, in the time win-

**Table 4.** Values of the parameters of Set1

Parameter	Set1	Unit
$N_1$	6.79E-06	1/m <sup>2</sup>
$N_2$	-7.74E-01	-
$N_3$	1.12E-08	-
$X_1$	2.06E-06	m
$X_2$	-5.45E-04	1/m
$X_3$	-1.96E02	m
$X_4$	-7.09E01	m
$Y_1$	-1.07E-02	1/m
$Y_2$	5.94E01	m
$Y_3$	1.19E01	m

dow between  $t_0 - 20$  s and  $t_0$  ( $t_w = 10$  s). As already said, the best initial velocity estimation is obtained in the middle of the time window, i.e.  $t_0 - t_w$ . The simulation will then cover the time interval from  $t_0 - 10$  s to  $t_0 + t_p$ , being  $t_p$  the time interval in which predicted data are needed. For example, a 40 s long simulation is needed to foresee a  $t_p = 30$  s. To compute the simulation, rudder position over time must be estimated since in principle they would be unknown in a real time application. Rudder angles are known from VDR data just for the first  $t_w$  seconds of simulation (i.e. from  $t_0 - 10$  s to  $t_0$ ). On the other hand, it is not possible to know the rudders position during the prediction period, i.e. from  $t_0$  to  $t_0 + t_p$ . The easiest solution would be to consider the rudder angles at  $t_0$  as a constant value for the whole simulation time. Anyway, this would lead to great errors if the rudder has not reached the ordered position at  $t_0$ . This is the reason why a more complex estimation procedure was chosen. The rudder angle set by the helmsman at  $t_0$  is compared with the actual rudder position. A linear ramp was then generated starting from actual position at  $t_0$  to the ordered position at  $t_0$ : ramp slope was evaluated by recorded navigation data (4.4°/s, in the case of Costa Concordia). Finally, when the ramp reaches the set angle position at  $t_1$ , rudder angle is kept constant for the interval between  $t_1$  and  $t_0 + 30$  s.

This procedure was tested on data recorded in the VDR for a given manoeuvre: Fig.8 shows the comparison between actual rudder angles and estimated ones. The black dashed line represents the ordered rudder position as recorded in the VDR, the black solid line represents the estimated rudder position during the foreseen period and the gray line represents the actual rudder position as recorded in the VDR. It is worth noting that the actual rudder position during the foreseen period (i.e. from  $t_0$  to  $t_0 + t_p$ ) would not be known in a real application. Obviously the plots are perfectly overlapped from  $t_0 - 10$  s to  $t_0$ . The estimation is still reliable between  $t_0$  and  $t_1$ , while some differences can be found after  $t_1$ , since no information are available about future ordered manoeuvres. Finally, Fig.8 highlights that the actual rudder position is limited to a maximum angle of 35° (e.g. for  $t \cong 20$  s), thus this limitation was also imposed to the predicted rudder position.

After rudder estimation was completed, the simulator was started to predict the trajectory in the chosen time interval. The position of the ship at the end of the prediction time could then be plotted on the electronic chart monitor available on the bridge. After each algorithm cycle (i.e. 1 s in the present work), the foreseen ship position was updated, taking into account any new manoeuvre ordered by the Commander and executed by the helmsman.

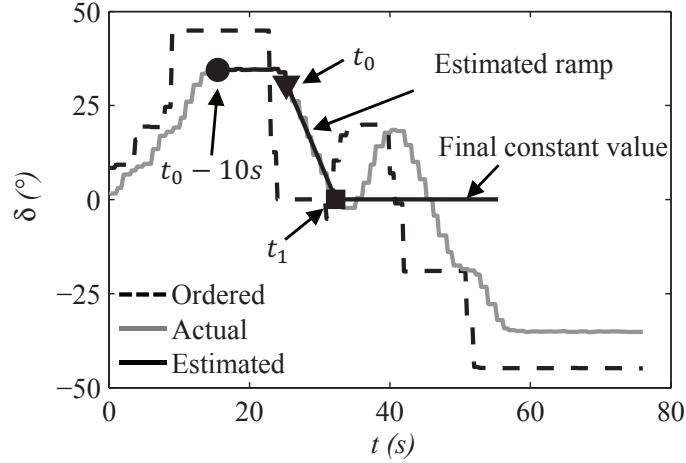


**Figure 8.** Rudder angles estimation for a known manoeuvre.

## 5.2. Results

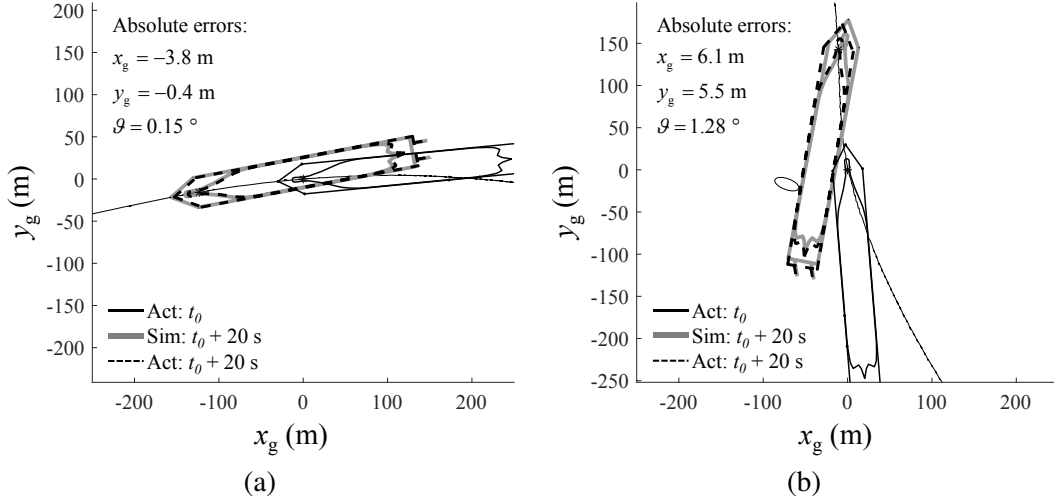
To evaluate the algorithm performances, it was applied to different recorded manoeuvres. This allowed to compare the foreseen final position with the actual one, recorded in the VDR files. In this way it was possible to check if initial conditions and rudder estimation procedures are reliable for prediction purposes. Since the exact rudder angles are not available for the great part of the simulation interval, but just estimated with the aforementioned procedure, results can not be as good as the ones obtained in the first part of the paper.

Fig.9 reports the comparison between the foreseen ship position and the recorded actual one for two different Costa Concordia manoeuvres near to Giglio island: the first was performed a few minutes before the impact (Fig.9(a)), and the second was performed just few seconds before the impact (Fig.9(b)). The estimation errors in Fig.9(a) are in the same order of magnitude of the GPS error, proving the reliability of the presented algorithm ( $t_p = 20$  s of predicted data are considered). Fig.9(b) is referred to a simulation performed in proximity of Giglio rocks (again,  $t_p = 20$  s). As can be seen, the error is greater in this latter case because of a discrepancy between the actual rudder angle and the estimated one. In fact, during the simulated time interval, a subsequent command was given 13 s after  $t_0$ , so that it could not be foreseen and considered in the prediction.

Fig.9(b) also shows that the proposed predictor would have helped the Commander to foresee the impact at least 20 s in advance, allowing to better plan evasive manoeuvres. Moreover, the simulator could highlight the helmsman's error before its effects were evident on ship's trajectory, allowing the Commander to correct it.

## 6. Conclusions

The present paper describes a time domain simulator for ship manoeuvring studies. The simulator is aimed at short time manoeuvres prediction (less than 80 s) because of the simplifying hypothesis introduced (e.g. environmental effects are neglected). It is complementary but does not substitute the a1 models, which are developed before ship construction and take into account all the design parameters. In the first part of the paper the proposed mathematical model was presented and the procedure to extract the needed constant parameters was described. An algorithm validation was also provided by simulating recorded manoeuvres and comparing



**Figure 9.** Predictor results for two different manoeuvres: (a) left turn and (b) Giglio rocks impact.

recorded position data with simulated ones. The results were really good, showing about 6 m of positioning error and less than  $2^\circ$  of heading error up to 40 s of simulation time, and a percentage error lower than 4 % up to 80 s of simulation. Also, simulation results comparison allowed to conclude that a reliable estimation of the model parameters can be achieved only by exploiting high accuracy navigation data, e.g. measured with a differential GPS system, or lower quality VDR data if properly filtered (e.g. through a Kalman filter). Despite the relatively short reliable simulation time, several applications were proposed for the methodology (after validating the approach on different ships), such as: forensic investigation of accidents, real time manoeuvres evaluation, auto-pilot control loop. More precisely, the proposed algorithm was applied to Costa Concordia shipwreck, to evaluate the effect of the helmsman's error on the trajectory of the ship which led to the impact with the rocks. Results showed that the impact could be avoided or, more likely, moved to a less dangerous location on the hull. Moreover, the impact energy could be decreased by about 75 %, reducing its catastrophic effects.

In the second part of the paper the proposed model was implemented in a real time fashion as a manoeuvres predictor. It was found that the predictor can be used to foresee ship's position due to certain order sequences, 40 s ahead in time (as long as no further manoeuvre are ordered by the Commander meantime, obviously). Results also showed that, in the case of Costa Concordia shipwreck, this predictor could foresee the impact with the rocks about 20 s ahead, giving a chance to avoid the impact and to correct the helmsman's error. At the present research stage the predictor can only be used as a support tool for simple manoeuvres evaluation. Further development could provide an interactive interface which could be used by the Commander to plan a series of rudder positions over time, in order to foresee and evaluate more complicated manoeuvres. On the other hand, this procedure could be time consuming and not suitable for emergency operations. Anyway, it could be implemented in an automatic tool which could try several different command sequences in a really short time, in order to provide the best manoeuvre suggestion to the Commander by choosing the best trajectory. Moreover, since the model showed its reliability in estimating ship's behaviour, it could be implemented in a controller for auto-pilot purposes or autonomous vehicles driving.

Future developments could be aimed at enhancing the data filtering strategy by exploiting a Kalman Filter (KF) method, which is widely adopted in this field Allotta et al. (2015b,a, 2016). This would allow to reduce recorded data noise level, obtaining higher quality veloc-

ity and acceleration estimation and thus improving the constant parameters computation (e.g. Set1 and Set2). Also, a more reliable estimation of initial conditions could be achieved exploiting a KF approach instead of the simpler polynomial interpolation. Also, a KF approach could be implemented in the simulation stage to foresee ship trajectory. This further step will be considered in future research and compared with the simpler forward Euler's method. It is worth noting that a reliable mathematical model is always needed in a KF approach, so the present research represents the first step for KF implementation. A further development could be represented by environmental effects modeling: the equation of motion could be modified by introducing wind and current effects through other constant parameters (i.e.  $N_{4,5}$ ,  $X_{5,6}$  and  $Y_{4,5}$ ) which could be computed using the navigation data recorded during the few seconds before the starting simulation time. The underlying mathematical model could also be improved in a future version of the simulator, to enhance its reliability for a longer time and to extend the application field of the method. A linear term in  $v$  could be added in the third of Eqs.2, to better represent the lift force acting on the hull in the case of low velocity along the transverse direction, and in the first of Eqs.2 to represent the yaw moment induced by the lift force. Another future enhancement could be achieved with a better description of the propellers effects: since the propeller thrust also depends on ship velocity  $u$ , a dependency between the propellers force and  $u$  could be added in the first and second of Eqs.2. Finally, the mathematical model could be further developed by considering the hydrodynamic force acting on the rudders in the second and third of Eqs.2 to represent its effect on acceleration along longitudinal and transverse directions.

### **Acknowledgment**

The author is grateful to CODACONS, an Italian consumers' rights association that participated to the trial for Costa Concordia shipwreck, for supporting this research.

## Nomenclature

VDR	Voyage Data Recorder.
CETENA	Centro per gli Studi di Tecnica Navale.
$x_g$	Horizontal global coordinate (fixed reference frame, east-west direction).
$y_g$	Vertical global coordinate (fixed reference frame, north-south direction).
$x$	Ship's longitudinal axis (moving reference frame).
$y$	Ship's transverse axis (moving reference frame).
$\vartheta$	Ship's heading, angle between $y_g$ and $x$ .
$u$	Ship's velocity along the longitudinal axis ( $\dot{x}$ ).
$v$	Ship's velocity along the transverse axis ( $\dot{y}$ ).
$U$	Ship's resultant translational velocity.
$r$	Ship's rotational velocity ( $\dot{\vartheta}$ ).
$\beta$	Ship's drift, angle between $x$ and $U$ .
$\delta$	Rudder angle.
$M_z$	Resultant yaw moment acting on the ship along $z$ axis.
$F_x$	Resultant force acting on the ship along $x$ axis.
$F_y$	Resultant force acting on the ship along $y$ axis.
$I_z$	Ship's moment of inertia along $z$ axis.
$m$	Ship's mass.
$p_1, p_2$	Propeller speed.
$N_i$	Constant parameters for Newton's equation along $z$ axis.
$X_i$	Constant parameters for Newton's equation along $x$ axis.
$Y_i$	Constant parameters for Newton's equation along $y$ axis.
$M_\vartheta$	Matrix form for Newton's equation along $z$ axis at different time instants.
$A^+$	Pseudoinverse of matrix $A$ .
$t_0$	Time at which the initial conditions need to be computed (simulation starting time).

$t_w$  Half length of the time window used to compute initial conditions.  
 $t_p$  Foreseen time for predictor application.  
 $a, b, c, d$  Coefficients of the polynomial interpolation for initial conditions calculation.  
 $d_t$  Integration time step.

## References

- 21st ITTC Manoeuvring Committee. 1996. Final report and recommendations to the 21st ittc. In: Proceedings of 21st ITTC; vol. 1. p. 347–398. Bergen - Trondheim, Norway.
- 22nd ITTC Manoeuvring Committee. 2002. Final report and recommendations to the 22nd ittc. In: Proceedings of 22nd ITTC. Seoul - Shanghai.
- 23rd ITTC Esso Osaka Specialist Committee. 2002. Final report and recommendations to the 23rd ittc. In: Proceedings of 23rd ITTC. Venice, Italy.
- 23rd ITTC Manoeuvring Committee. 2002. Recommended Procedures-Testing and Extrapolation Methods -Manoeuvrability Validation of Manoeuvring Simulation Models. Available from: [http://www.simman2008.dk/PDF/7.5-02-06-03%20\(simulation%20models\).pdf](http://www.simman2008.dk/PDF/7.5-02-06-03%20(simulation%20models).pdf).
- Allotta B, Caiti A, Chisci L, Costanzi R, Di Corato F, Fantacci C, Fenucci D, Meli E, Ridolfi A. 2015a. Development of a navigation algorithm for autonomous underwater vehicles. *IFAC-PapersOnLine*. 28(2):64–69.
- Allotta B, Caiti A, Costanzi R, Fanelli F, Fenucci D, Meli E, Ridolfi A. 2016. A new auv navigation system exploiting unscented kalman filter. *Ocean Engineering*. 113:121–132.
- Allotta B, Chisci L, Costanzi R, Fanelli F, Fantacci C, Meli E, Ridolfi A, Caiti A, Di Corato F, Fenucci D. 2015b. A comparison between ekf-based and ukf-based navigation algorithms for auvs localization. In: *OCEANS 2015*.
- Barauskis G, Friis-Hansen P. 2007. Fast-time ship simulator. In: *Safety at Sea*.
- Bums RS. 1995. The use of artificial neural networks for the intelligent optimal control of surface ships. *IEEE JOURNAL OF OCEANIC ENGINEERING*. 20(1).
- Das S, Talole SE. 2016. Robust steering autopilot design for marine surface vessels. *IEEE JOURNAL OF OCEANIC ENGINEERING*. 41(4).
- Epperson JF. 2013. *An introduction to numerical methods and analysis*, 2nd edition. Wiley.
- Gubian P, Piccinelli M, Neri P, Neri B, Giurlanda F. 2015. The disaster of costa concordia cruise ship: an accurate reconstruction based on black box and automation system data. In: *2nd International Conference on Information and Communication Technologies for Disaster Management, ICTDM 2015*.
- InternationalMaritimeOrganization IMO. 1997. PERFORMANCE STANDARDS FOR SHIPBORNE VOYAGE DATA RECORDERS (VDRs). Resolution A.861(20), adopted on 27 November 1997; Available from: <http://www.imo.org/>.
- Ishiguro T, Tanaka S, Yoshimura Y. 1996. A study on the accuracy of the recent prediction technique of ship's manoeuvrability at an early design stage. In: *Proceedings of Marine Simulation and Ship Manoeuvrability*. Copenhagen, Denmark.
- Lawson CL, Hanson RJ. 1995. *Solving least squares problems*. siam. Classics in Applied Mathematics.
- Maffezzoni P, Gubian P. 1995. A new unsupervised learning algorithm for the placement of centers in a radial basis function neural network (rbfn). In: *Proceedings of 1995 International Conference on Neural Networks*. p. 1258–1262. Perth, Western Australia.
- Maimun A, Priyanto A, Muhammad A, Scully C, Awal Z. 2011. Manoeuvring prediction of pusher barge in deep and shallow water. *Ocean Engineering*. 38:1291–1299.
- Maimun A, Priyanto A, Rahimuddin, Sian A, Awal Z, CS CC, Nurcholis, Waqiyuddin M. 2013. A mathematical model on manoeuvrability of a lng tanker in vicinity of bank in restricted water. *Safety Science*. 53:34–44.
- Martelli M, Viviani M, Altosole M, Figari M, Vignolo S. 2014. Numerical modelling of propulsion, control and ship motions in 6 degrees of freedom. *Journal of Engineering for the Maritime Environment*. 228:373–397.
- McMahon J, Plaku E. 2016. Mission and motion planning for autonomous underwater vehicles operating in spatially and temporally complex environments. *IEEE JOURNAL OF OCEANIC ENGINEERING*. 41(4).
- Milanov E, Chotukova V, Stern F. 2011. Experimental and simulation studies on fast delft372 catamaran maneuvering and course stability in deep and shallow water. In: *Proceedings of 11th International Conference on Fast Sea Transportation, FAST 2011*. Honolulu, Hawaii, USA.
- Mohd N, Wan N, Mamat M. 2012. Ship manoeuvring assessment by using numerical simulation ap-

- proach. *Journal of Applied Sciences Research*. 8:1787–1796.
- Neri P, Neri B. 2015. A short term simulator for vessel manoeuvres prediction. In: *Proceedings of ApplePies 2015*. Rome, Italy.
- Neri P, Piccinelli M, Gubian P, Neri B. 2014. A ship motion short term time domain simulator and its application to costa concordia emergency manoeuvres just before the january 2012 accident. In: *28th European Conference on Modelling and Simulation, ECMS 2014*, p. 64–70. Brescia, Italy.
- Oltmann P. 1996. On the influence of speed on the manoeuvring behaviour of a container carrier. In: *Proceedings of Marine Simulation and Ship Manoeuvrability*. Copenhagen, Denmark.
- Piccinelli M, Gubian P. 2013. Modern ships voyage data recorders: a forensics perspective on the costa concordia shipwreck. *Digital investigation*. 10.
- Poggio T, Girosi F. 1990. Networks for approximation and learning. In: *Proceedings of the IEEE*. p. 1481–1497.
- Pérez T, Blanke M. 2002. Simulation of ship motion in seaway. Technical University of Denmark. Report No.:
- Raman-Nair W, Gash R, Sullivan M. 2014. Effect of wind and current on course control of a maneuvering vessel. In: *Oceans - St. John's, 2014*. IEEE. p. 1–5. St. John's, NL, Canada.
- Revestido E, Velasco F, Zamanillo I, López E, Moyano E. 2011. Parameter estimation of ship linear maneuvering models. In: IEEE, editor. *Proceedings of Oceans 2011*. Spain.
- Sandaruwan D, Kodikara N, Keppitiyagama C, Rosa R. 2010. A six degrees of freedom ship simulation system for maritime education. *The International Journal on Advances in ICT for Emerging Regions*:pp 34–47.
- Shyh-Kuang U, Lin D, Chieh-Hong L. 2008. A ship motionsimulation system. *Springer-Verlang Virtual Reality*:65–76.
- Skjetne R, Smogeli N, Fossen T. 2004. A nonlinear ship manoeuvring model: Identification and adaptive control with experiments for a model ship. *MODELLING, IDENTIFICATION AND CONTROL*. 25(1):3–27.
- Suleiman BM. 2000. Identification of finite-degree-of-freedom models for ship motions [dissertation]. Virginia Polytechnic Institute and State University.
- Sutulo S, and C Guedes Soares LM. 2002. Mathematical models for ship path prediction in manoeuvring simulation systems. *Ocean Engineering*. Vol. 29:1–19.
- Varela J, Soares CG. 2015. Interactive 3d desktop ship simulator for testing and training offloading manoeuvres. *Applied Ocean Research*. 51:367–380.

## Appendix A. Regression analysis results

Since the proposed model is based on the computation of the parameter Set1 through the least square fit of data recorded during the Turning circle manoeuvre C1, the results of the performed regression analysis are reported below for the three considered quantities, i.e. the rotational acceleration  $\ddot{\vartheta}$ , Fig.A1, the linear acceleration  $\ddot{x}$ , Fig.A2, and the linear acceleration  $\ddot{y}$ , Fig.A3. The black dots in the figures represent the recorded data, while the gray line represents the least square fit obtained with the proposed procedure. It is worth noting that at the beginning of the manoeuvre the ship undergoes a transient regime due to the change of the trajectory radius, thus an acceleration along the  $x$  and  $y$  directions was found, along with a rotational acceleration. The results show a really good agreement between the data measured during the sea trial and their least square fit, for all the considered quantities.

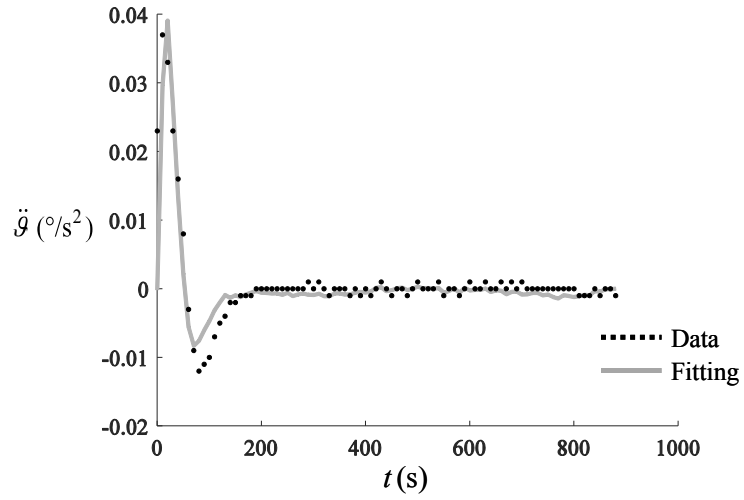


**Figure A1.** Set1 computation, regression analysis for the rotational acceleration  $\ddot{\vartheta}$ .

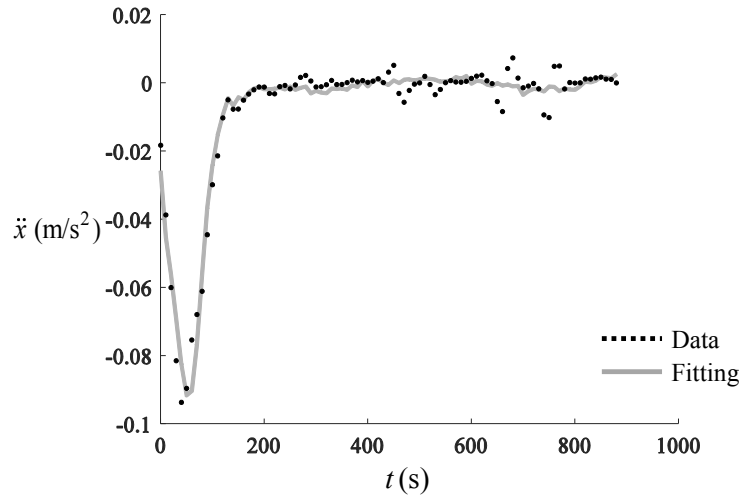


**Figure A2.** Set1 computation, regression analysis for the linear acceleration  $\ddot{x}$ .

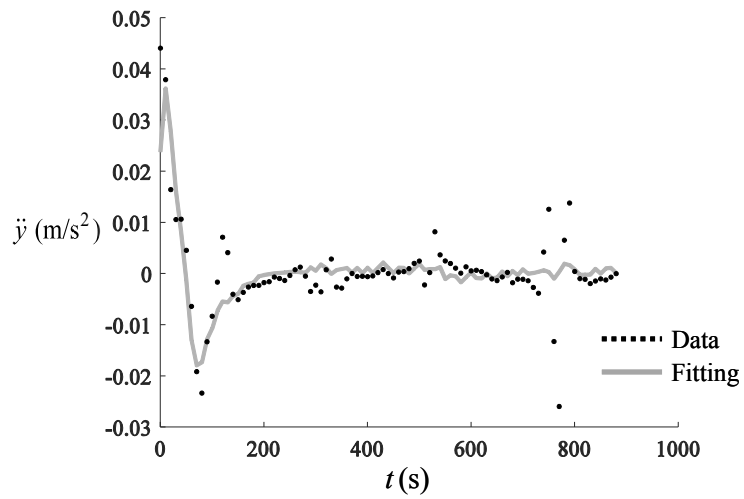


**Figure A3.** Set1 computation, regression analysis for the linear acceleration  $\ddot{y}$ .

## Appendix B. Model validation results

The proposed model was validated through the comparison between recorded and simulated data during different manoeuvres. Some numerical results are reported in Tab. 2, in terms of absolute and relative simulation errors. The following figures expand these comparisons. Figure B1 represents an extended view of the trajectory of the ship corresponding to Giglio Impact manoeuvre V1, Palamos Turn manoeuvre V2 and Palma Zig-Zag manoeuvre V3 (Fig. B1(a), (b) and (c) respectively). Figures B2, B3 and B4 show a zoomed view of the comparison for the Palamos Turn manoeuvre V2, for a simulation time of 20 s, 40 s and 80 s respectively (using parameter Set1). The left side of the figures show the full simulation path, while the right side of the figures show a zoomed view of the ship. The solid line refers to the measured trajectory, while the dashed line is referred to the simulated portion of the trajectory. Position and orientation as recorded in the VDR are represented with a black line, while the simulated ones are represented with a gray line. As can be seen, both measured and simulated data are almost overlapped for 20 s and 40 s simulations, while discrepancies can be noted for the 80 s simulation, as reported in Tab. 2.

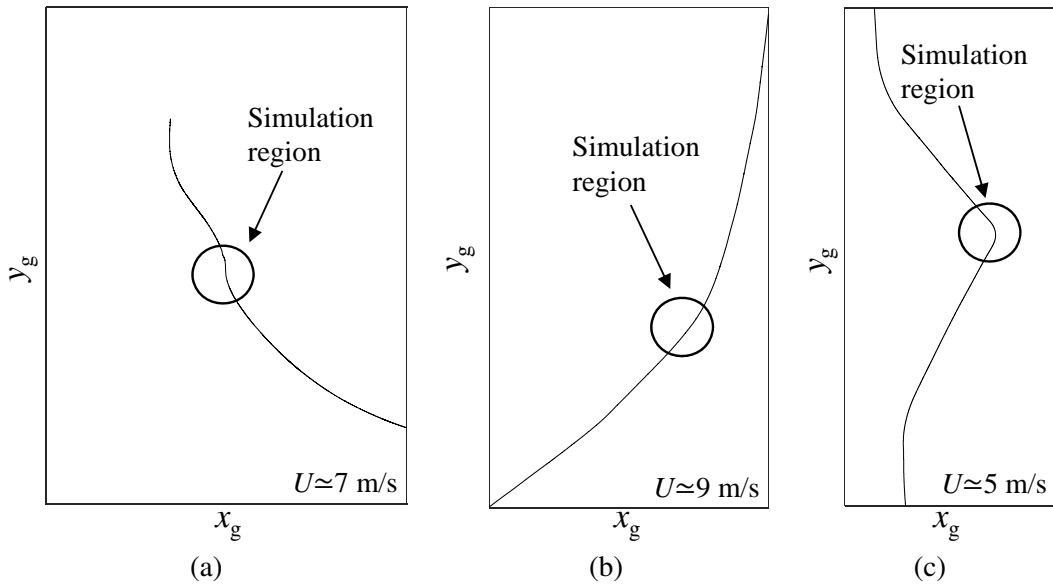


**Figure B1.** Complete trajectory corresponding to validation manoeuvres: (a) Giglio Impact V1, (b) Palamos Turn V2 and (c) Palma Zig-Zag V3.

On the other hand, Figs. B5, B6 and B7 report the zoomed view of the Palma Zig-Zag manoeuvre V3, for a simulation time of 20 s, 40 s and 80 s respectively (using parameter Set1). Again, measured and simulated data are almost overlapped for 20 s and 40 s simulations, while some discrepancies can be noted for the 80 s simulation, as highlighted in Tab. 2. These results further confirm that the proposed simulator is reliable for short time simulation up to 40 s, while simulation accuracy decreases for longer simulation time.

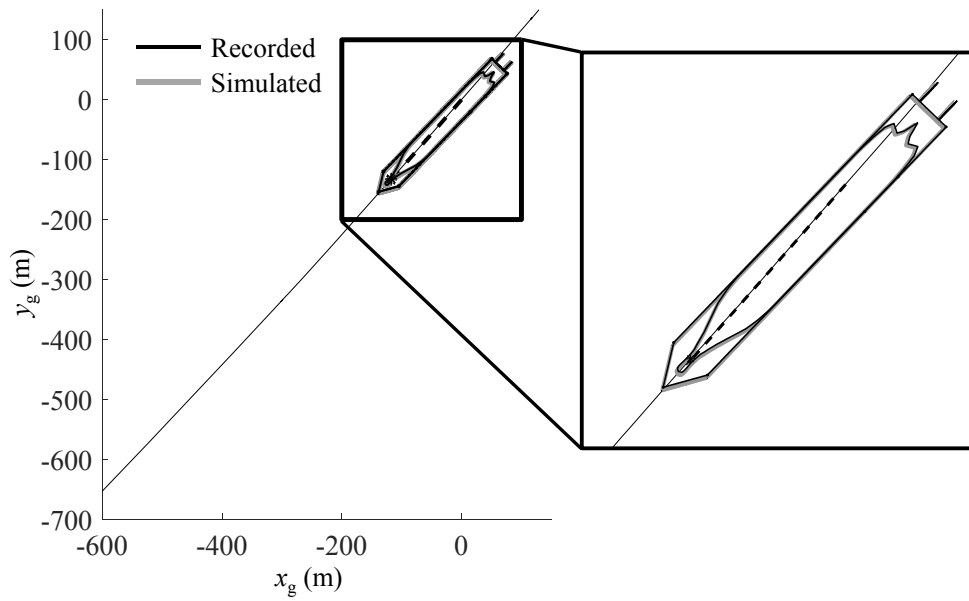


**Figure B2.** Simulation results for the Palamos Turn manoeuvre V2, simulation time 20 s.

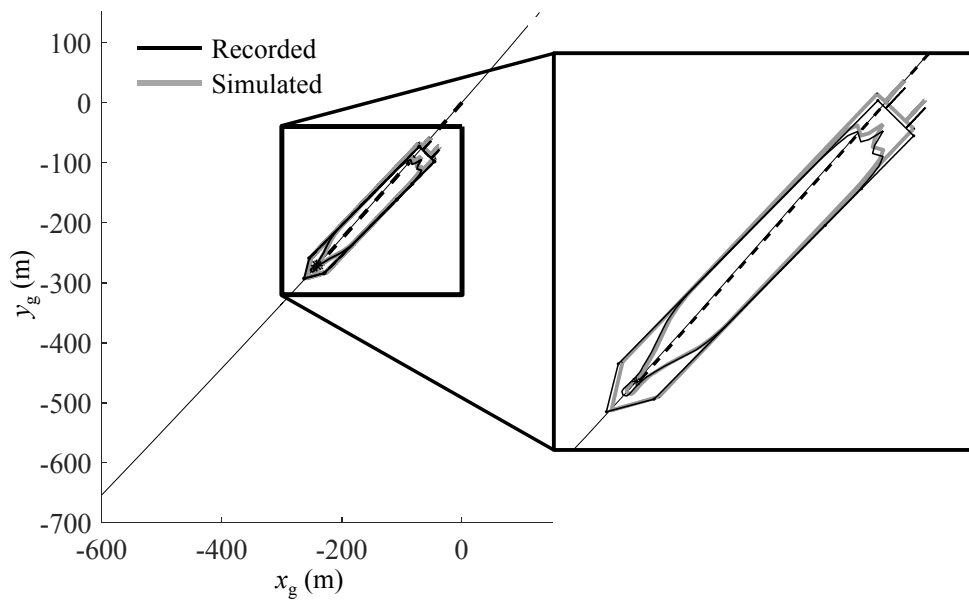


**Figure B3.** Simulation results for the Palamos Turn manoeuvre V2, simulation time 40 s.

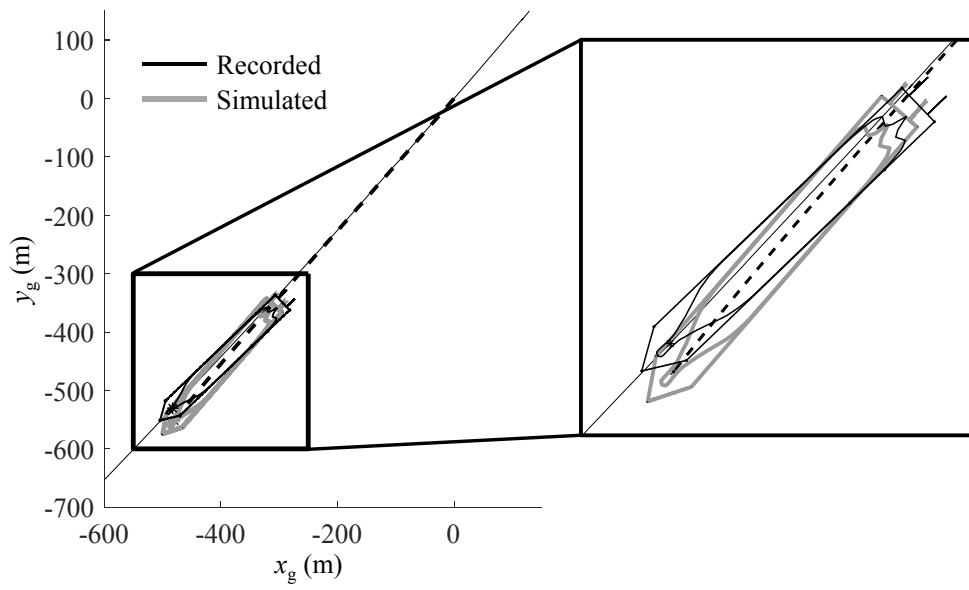


**Figure B4.** Simulation results for the Palamos Turn manoeuvre V2, simulation time 80 s.

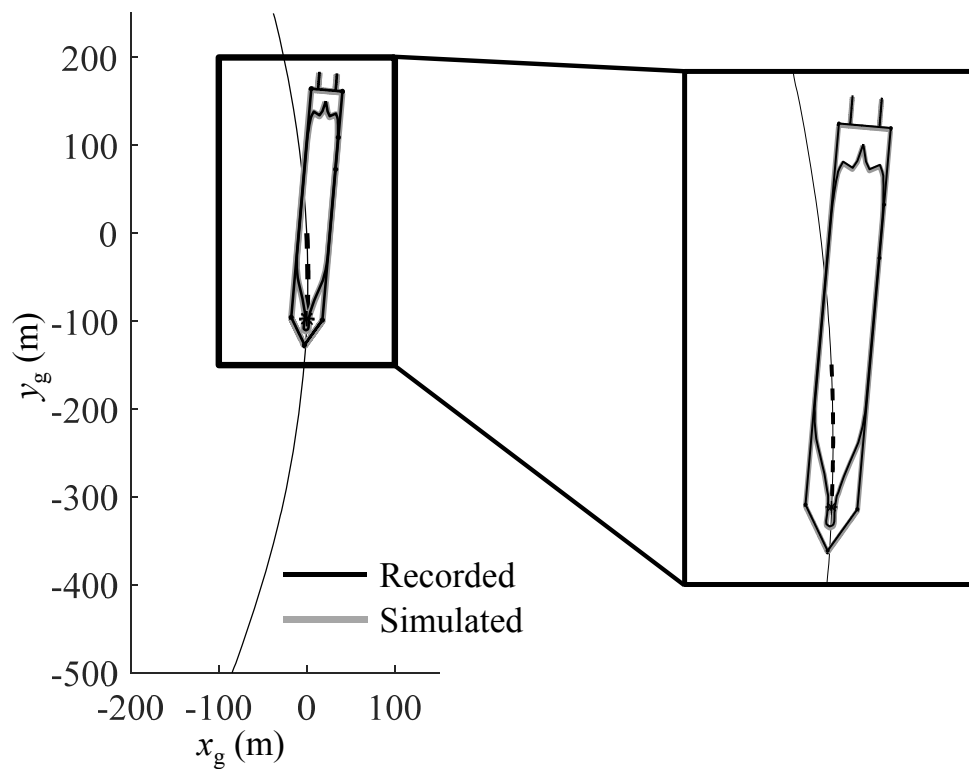


**Figure B5.** Simulation results for the Palma Zig-Zag manoeuvre V3, simulation time 20 s.

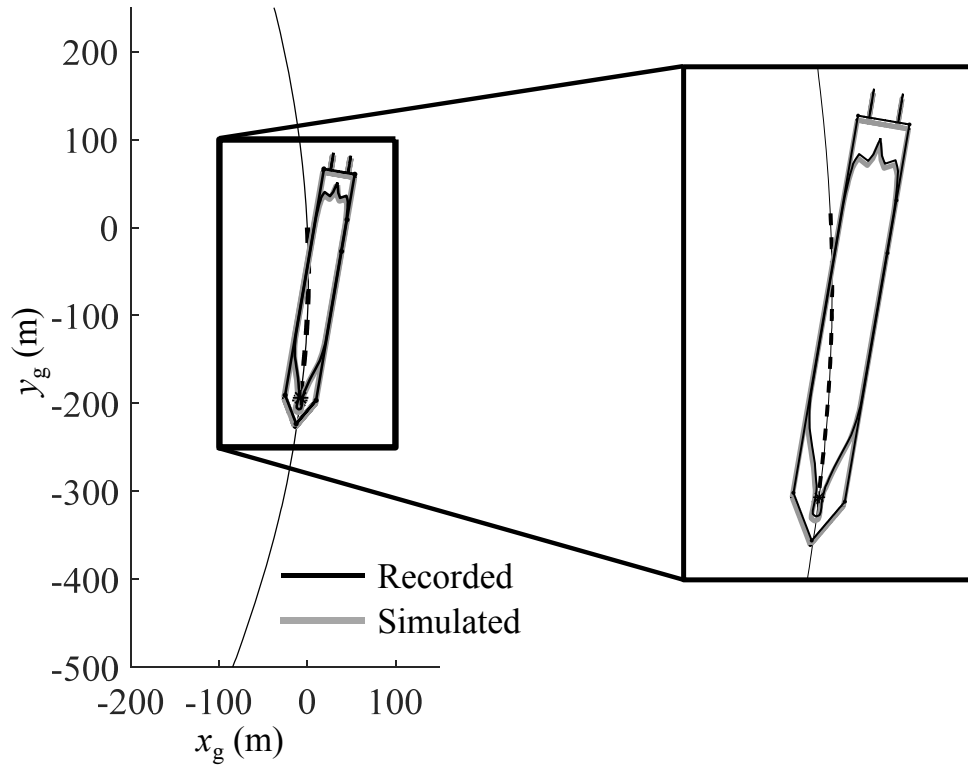


**Figure B6.** Simulation results for the Palma Zig-Zag manoeuvre V3, simulation time 40 s.

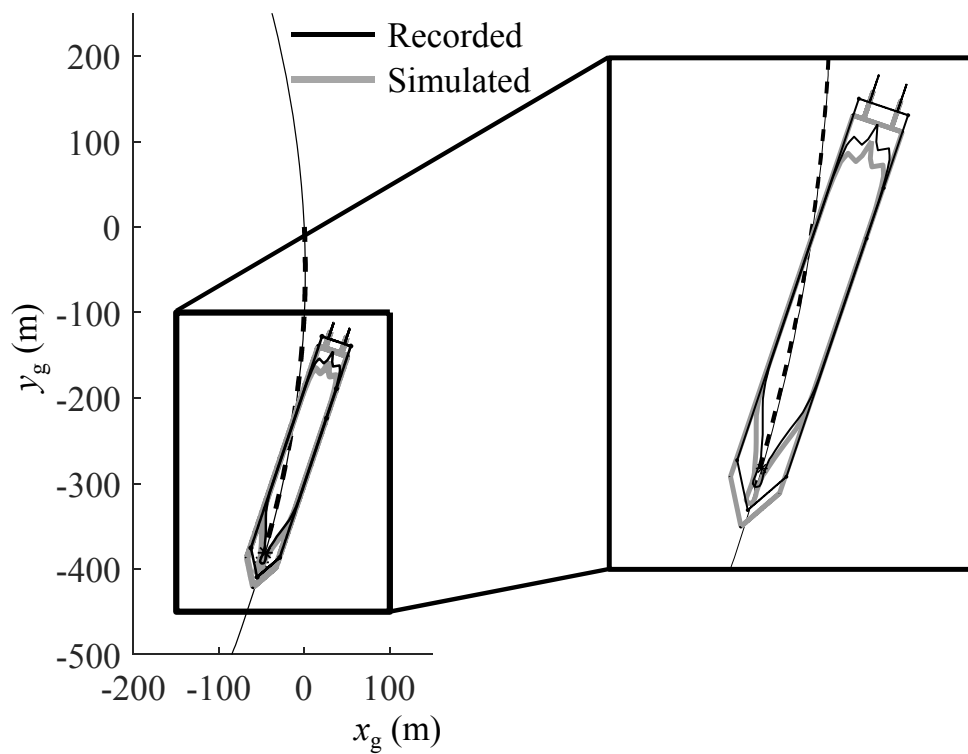


**Figure B7.** Simulation results for the Palma Zig-Zag manoeuvre V3, simulation time 80 s.